Improved catalytic activity of $Mo_{1-x}W_xSe_2$ alloy nanoflowers promotes efficient hydrogen evolution reaction in both acidic and alkali aqueous solutions

Electronic Supporting Information

Oren E. Meiron,[a] Vasu Kuraganti,[a] Idan Hod[a], Ronen Bar-Ziv[a,b] and Maya Bar-Sadan[a,*]

[a] Ben-Gurion University of the Negev, Department of Chemistry, Beer-Sheva

[b] Nuclear Research Center Negev, Beer-Sheva 84190, Israel.

[*] Corresponding author: **barsadan@bgu.ac.il**

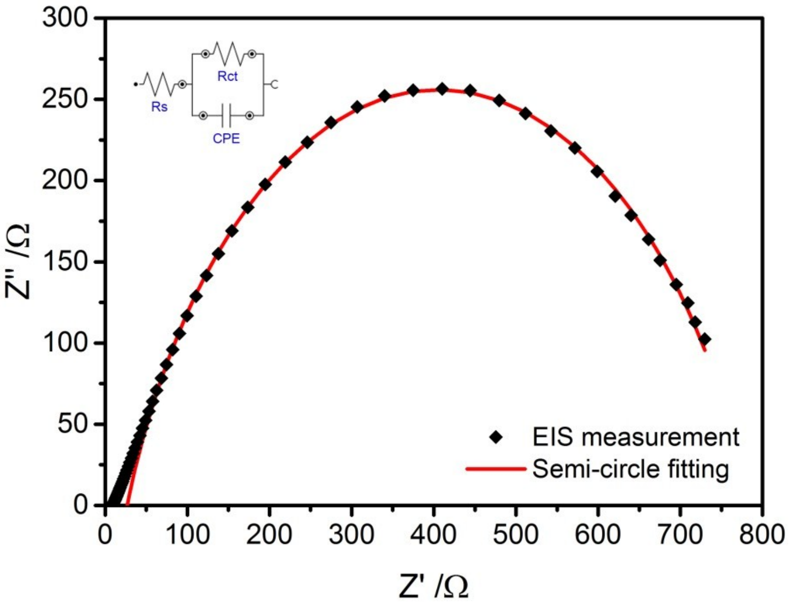

Figure S1. EIS measurement and semi-circle fitting of $Mo_{0.57}W_{0.43}Se_2$ at 200 mV overpotential. The fitting was performed according to the circuit provided in the upper left corner (Rs, series resistance. Rct, charge-transfer resistance. CPE, constant phase element for chemical capacitance).

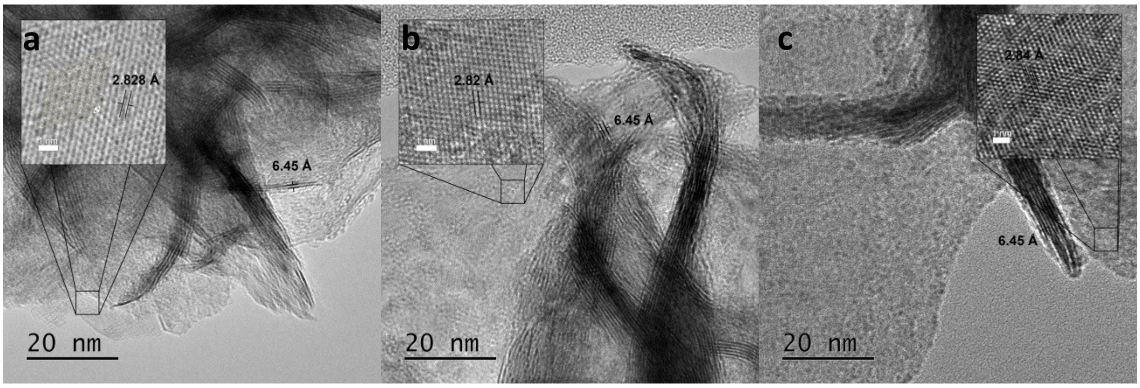

Figure S2. HRTEM images and inter-planar spacing of (a) $MoSe_2$, (b) $Mo_{0.57}W_{0.43}Se_2$ and (c) WSe_2. Insets show high resolution images of the 100 plane. Inter-planar spacing was extracted from FFT.

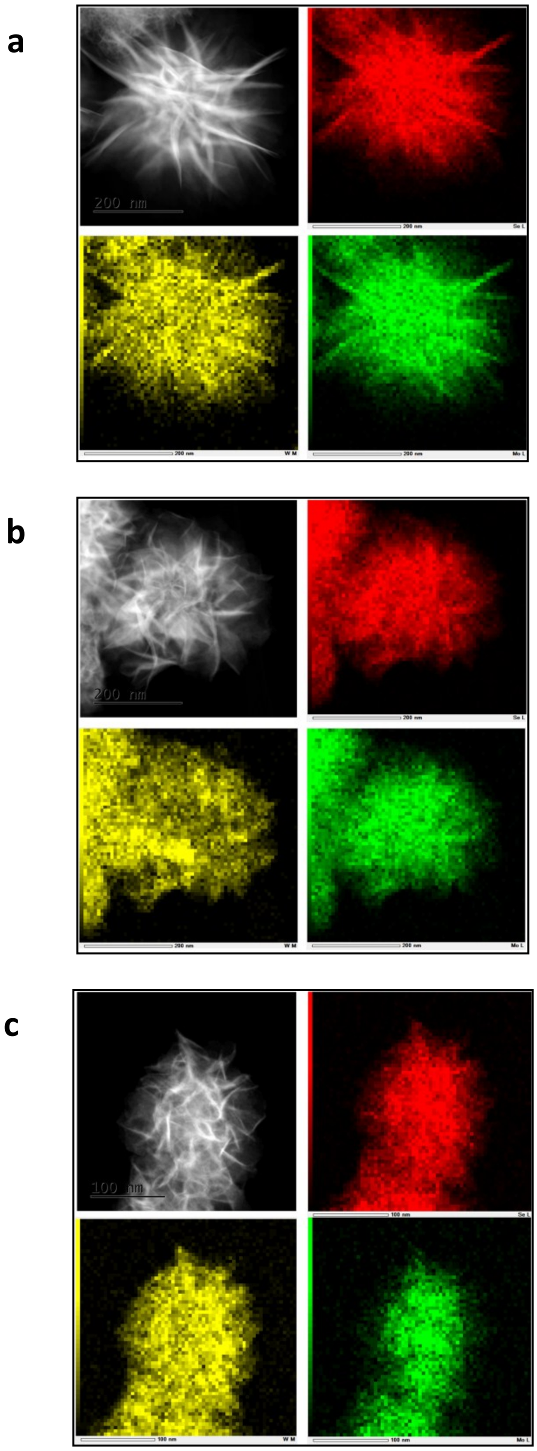

Figure S3. HAADF-STM and EDS maps of $Mo_{1-x}W_xSe_2$ alloys. The maps show the presence of both Mo and W in (a) $Mo_{0.75}W_{0.25}Se_2$, (b) $Mo_{0.57}W_{0.43}Se_2$ and (c) $Mo_{0.25}W_{0.75}Se_{2.}$ Red = Se, green = Mo and Yellow = W.

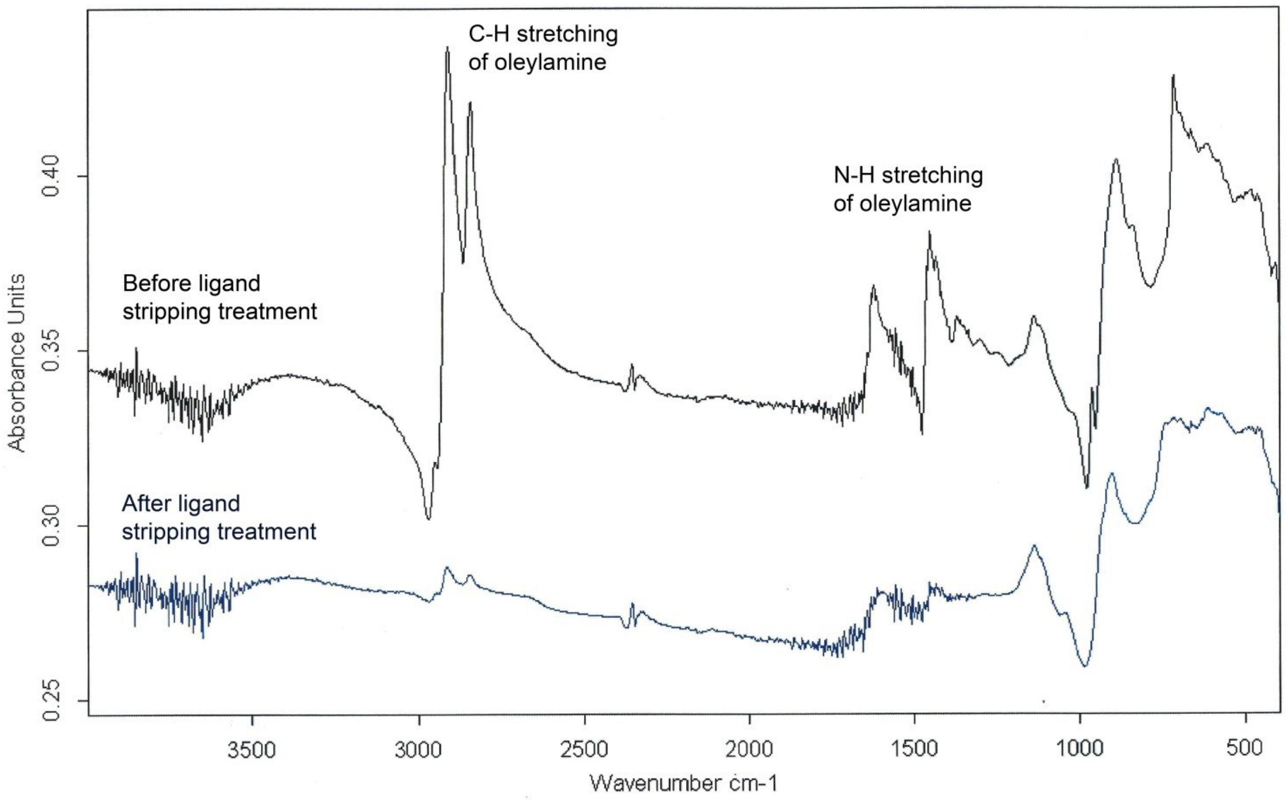

Figure S4. ATR-FTIR spectra of typical alloys before (black line) and after (dark blue line) ligand stripping treatment, showing a reduction of more than 90% in the oleylamine capping ligands.

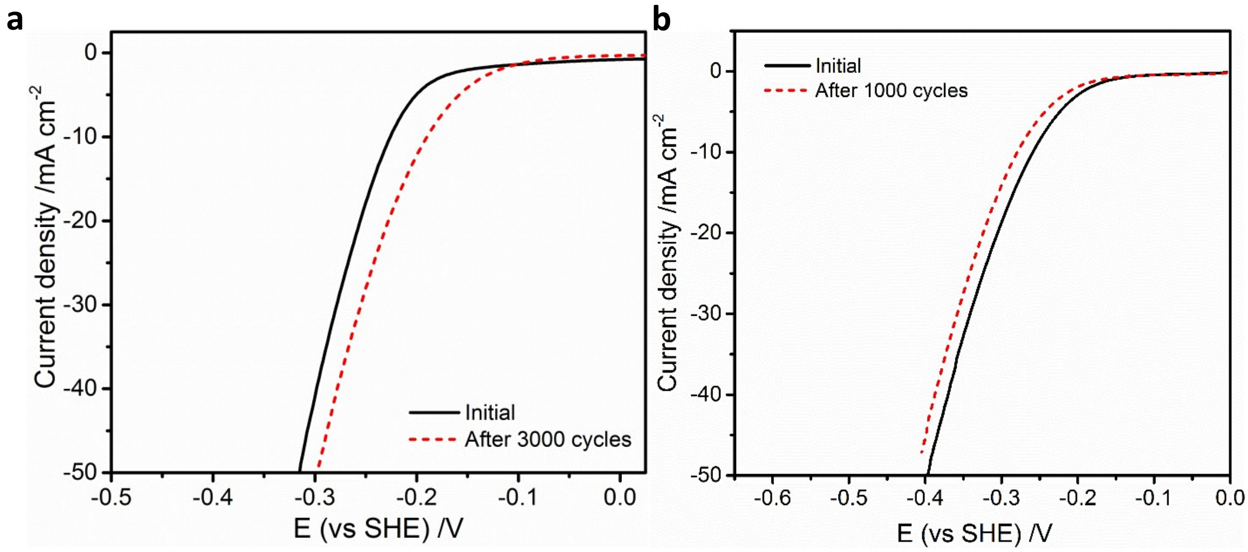

Figure S5. Stability analysis of $Mo_{1-x}W_xSe_2$ alloys. (a) Stability analysis of $Mo_{0.57}W_{0.43}Se_2$ in acid and (b) Stability analysis of $Mo_{0.75}W_{0.25}Se_2$ in alkaline solution. The electrode was cycled between -400 to 100 mV (vs SHE) at a scan rate of 100 mV/sec under Ar.

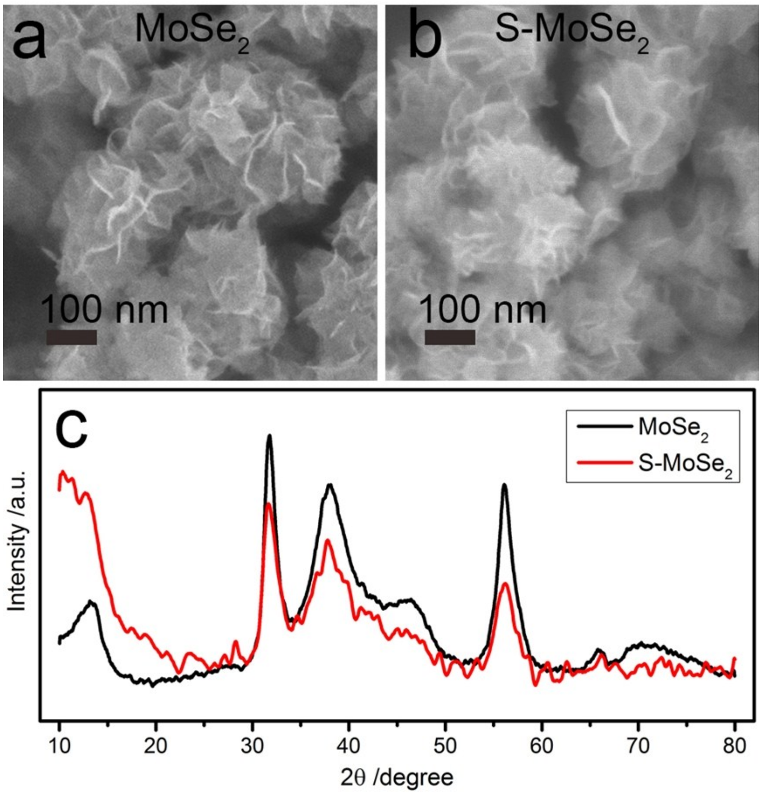

Figure S6. Comparison between MoSe$_2$ produced by two synthetic procedures. SEM images of (a) MoSe$_2$ nanoflowers produced by the procedure described herein, (b) S-MoSe$_2$ nanoflowers produced by an alternative procedure and (c) XRD spectra of the two MoSe$_2$ nanoflowers normalized to AUC.

Table S1. Elemental analysis from XPS spectra. The elemental calculation error is ± 1 % for all the results.

		Feed ratio		From XPS		
		Mo	W	Mo	W	Ratio
MoWSe	x=0.00	1.00	0.00	1.00	0.00	0.00
	x=0.25	0.75	0.25	0.75	0.25	0.25
	x=0.43	0.50	0.50	0.57	0.43	0.43
	x=0.75	0.25	0.75	0.25	0.75	0.75
	x=1.00	0.00	1.00	0.00	1.00	1.00

Table S2. Electrochemical analysis comparison between $MoSe_2$ and S-$MoSe_2$

	Acid		Alkaline	
	η [mV] at 10 mA cm^{-2}	Tafel from polarization curves [mV/dec]	η [mV] at 10 mA cm^{-2}	Tafel from polarization curves [mV/dec]
$MoSe_2$ (this work)	243	93	310	114
S-$MoSe_2$	205	73	260	96

Table S3. Elemental analysis of $MoSe_2$ and S-$MoSe_2$ showing the different Mo/Se ratio.

	Mo /%	Se /%	**Ratio**
$MoSe_2$	35±1	64±1	**1.83**
S-$MoSe_2$	33±1	67±1	**2.03**

Table S4: The HER activity of the $Mo_{0.57}W_{0.43}Se_2$, $MoSe_2$ and S-$MoSe_2$ and the reported TMD-based catalysts.

Catalyst	**Overpotential (mV) at 10 mA/cm²**	**Tafel slope (mV/decade)**	**Electrolyte**	**Comment**
$Mo_{0.57}W_{0.43}Se_2$	209	76	0.5M H_2SO_4	Current work
$Mo_{0.75}W_{0.25}Se_2$	262	101	0.5M KOH	
$MoSe_2$	243	93	0.5M H_2SO_4	
S-$MoSe_2$	205	73	0.5M H_2SO_4	
Defect rich MoS_2[7]	120 (onset at -1 mA/cm²)	50	0.5M H_2SO_4	
Double-gyroid MoS_2[8]	150-200 (onset at -1 mA/cm²)	50	0.5M H_2SO_4	
$MoSe_2$ nanoflowers[10]	300 (at -13 mA/cm²)	98	0.5M H_2SO_4	
WS_2[16]	~230 (at -2 mA/cm²)	-	Acid	
$MoS_{1.7}Se_{0.3}$ Nanobelts[17]	139 (at -20 mA/cm²)	65	0.5M H_2SO_4	
$W(S_{0.48}Se_{0.52})_2$[18]	-	99	1M H_2SO_4	iR corrected
$MoS_{1.0}Se_{1.0}$[19]	-	56	0.5M H_2SO_4	
$Mo_{0.5}W_{0.5}Se_2$[20]	107 (at -1 mA/cm²)	57	Acid	
$MoSe_2$[20]	112	44	Acid	
Ni-MoS_2[24]	98	60	1M KOH	
Amorphous MoS_x films[24]	540 (at 4 mA/cm²)	-	0.1M KOH	
MoS_3 Low loading[34]	250 (at -20 mA/cm²)	47	1M H_2SO_4	
MoS_3 high loading[34]	240 (at -20 mA/cm²)	63	1M H_2SO_4	